Probing of Lipase Activity at Air/Water Interface by Sum-Frequency Generation Spectroscopy

Gediminas Niaura,*,† Zenonas Kuprionis,‡ Ilja Ignatjev,† Marytė Kažemėkaitė,† Gintaras Valincius,† Zita Talaikytė,† Valdemaras Razumas,† and Allan Svendsen§

Institute of Biochemistry, Mokslininkų 12, LT-08662 Vilnius, Lithuania, EKSPLA Ltd., Savanorių Av. 231, LT-02300 Vilnius, Lithuania, and Novozymes A/S, Smørmosevej 25, DK-2880 Bagsvaerd, Denmark

Received: July 27, 2007; In Final Form: December 20, 2007

The infrared-visible sum-frequency generation (SFG) vibrational spectroscopy was used to probe enzymatic activity of *Thermomyces lanuginosus* lipase (TLL) at air/water interface. A monolayer of amphiphilic O-palmitoyl-2,3-dicyanohydroquinone (PDCHQ), containing target ester group and two CN groups serving as vibrational markers, was utilized as an enzyme substrate. SFG data revealed the detailed molecular scale structure and properties of the PDCHQ layer at the interface. In particular, we demonstrate that hydrophilic headgroup of PDCHQ is mainly in the form of an oxyanion, and the enzyme-induced cleavage of the ester bond could be spectroscopically monitored by the disappearance of the intense C≡N resonance at 2224 cm^{-1}. The enzymatic nature of the ester bond cleavage was confirmed by the control experiments with deactivated S146A mutant variant of TLL. By comparing action of wild type (WT) TLL and its inactive S146A mutant, it was shown that two effects take place at the interface: disordering of the lipid monolayer due to the adsorption of enzyme and enzymatic cleavage of the ester bond. The concentration of enzyme as low as 10 nM could be easily sensed by the SFG spectroscopy. We present spectroscopic evidence that upon hydrolysis one of the products, 2,3-dicyanohydroquinone, leaves the surface, while the other, palmitic acid, remains at air/water interface in predominantly undissociated form with the mono-hydrogen-bonded carbonyl group. Strong amide I (1662 cm^{-1}) and amide A (3320 cm^{-1}) SFG signals from TLL suggest that enzyme molecules position themselves at air/water interface in an orderly fashion. Presented work demonstrates the potential of SFG spectroscopy for in situ real-time monitoring of enzymatic processes at air/water interface.

1. Introduction

Important biocatalytic reactions associated with transformations of lipids take place at interfaces.[1−3] The rate of these reactions critically depends on the lipid layer structure, interaction of enzyme with the amphiphilic compounds, and surface-induced conformational changes of enzymes.[2,3] To understand and control biocatalytic processes at surfaces, detailed molecular level information on organization of interface is required. Most of the traditional methods for investigation of air/liquid interface yield macrolevel physical and chemical information or lack required interfacial sensitivity. Among the experimental techniques suitable for such studies, vibrational sum-frequency generation (SFG) spectroscopy seems particularly attractive because of molecular specificity and intrinsic interfacial sensitivity.[4−6] Surface sensitivity of the technique arises from the fact that within the electric dipole approximation the nonlinear generation of the sum-frequency (SF) signal from the overlapped visible and infrared beams is forbidden in the media of randomly oriented molecules or in the centrosymmetric media but is allowed at the interface where inversion symmetry is broken.[5,6] Molecular specificity emerges from the ability to record vibrational spectrum. Consequently, a number of unique physical phenomena were recently explored by SFG vibrational spectroscopy from the films at the air/water interface. Among them are the conformational changes in phospholipid monolayers,[7] phase transition thermodynamics in monomolecular films,[8] positioning of the surfactants[9] as well as protein and peptide adsorption at air/water interface.[10−12]

In this work, the first application of SFG spectroscopy for monitoring enzymatic process at air/water interface is described. The enzyme we have chosen was *Thermomyces lanuginosus* lipase (TLL), which belongs to the triglyceride hydrolase (EC 3.1.1.3) class of enzymes. Lipases act on water-insoluble substrates, catalyzing the hydrolysis of the ester bond.[1−3] They also hydrolytically digest alicyclic and aromatic esters and therefore have a variety of industrial applications.[3] The catalytic activity of lipases may increase orders of magnitude once the enzyme is bound to the surface of water-insoluble substrates. The mechanism of interfacial activation is still under debate; however, in case of TLL the activation is related to the conformational change of the protein surface domain, which leads to the exposure of the catalytic triad consisting of Ser, His, and Asp/Glu to substrate.[3] A challenging problem in elucidating the catalytic mechanism of lipases in general and TLL in particular is related to the fact that the traditional enzymatic activity measurements (e.g., pH-stat titration) are obstructed by polymorphism and complexity of organization state of aggregated substrates (e.g., triglycerides), which under the experimental conditions is impossible to control.[13] Poorly water-soluble substrates form monomers and micelles, chunk aggregates and adsorb on vessel walls as well as on the air−

* To whom correspondence should be addressed. Phone: +3705 272 9642. Fax: +3705 272 9196. E-mail: gniaura@ktl.mii.lt.
† Institute of Biochemistry.
‡ EKSPLA Ltd.
§ Novozymes A/S.

10.1021/jp075950m CCC: $40.75
Published on Web 03/07/2008

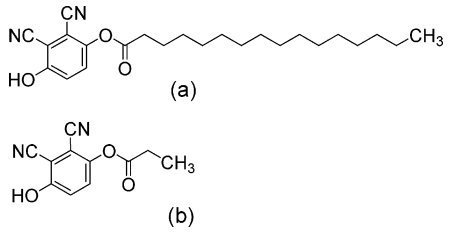

Figure 1. Molecular structures of PDCHQ (a) and model compound DCHPP used in calculations (b).

water interface; therefore, measured enzyme activity is the sum of different contributions that hampers the data and makes it difficult to resolve the mechanism of an enzymatic action.[13] From this perspective, SFG vibrational spectroscopy may offer an alternative that allows to avoid aforementioned difficulties because the recorded enzyme activity signal in this case is generated only by the organized surface layer of substrate and enzyme at air−water interface. Therefore, the main objective of the current work was to directly detect enzymatic activity of a lipase (TLL) and to characterize the molecular environment of the interface in which the hydrolysis takes place. For this purpose, we used custom synthesized substrate O-palmitoyl-2,3-dicyanohydroquinone (PDCHQ, Figure 1a), which as we showed earlier[14] is enzymatically cleaved by the lipase. One could expect that CN-groups of PDCHQ spread at air/water interface will generate a strong SFG signal in the 2200−2300 cm^{-1} frequency region. Indeed, in this work, we observed intense band at 2242 cm^{-1} in both infrared and Raman spectra of solid PDCHQ in accordance with general requirement for generation of strong SF resonance.[15] Because the hydrolysis yields water soluble 2,3-dicyanohydroquinone, the lipase injection into the system should trigger the CN band decay, thus allowing it to directly monitor lipase activity by the SFG vibrational spectroscopy.

2. Experimental Section

SF spectra were recorded using EKSPLA (Vilnius, Lithuania) picosecond SFG spectrometer. The spectrometer is based on a mode-locked EKSPLA PL2143A/20 Nd:YAG laser generating 28 ps pulses at 1064 nm with 20 Hz repetition rate. In some experiments, EKSPLA PL2143A/50 Nd:YAG laser-generating pulses with 50 Hz repetition rate was employed. The second harmonic radiation (wavelength 532 nm, pulse energy 300−400 μJ) from this laser was used as a visible beam (ω_{VIS}). The tunable infrared pulses (ω_{IR}) in the 1500−3750 cm^{-1} frequency region with the energies of 80−200 μJ were produced in parametric generator EKSPLA PG401VIR/DFG pumped by third harmonic (355 nm) and fundamental radiation of the laser. The bandwidth of ω_{IR} was <6 cm^{-1}. To produce SFG spectra, the ω_{IR} and ω_{VIS} beams were incident at angles of 53 and 60°, respectively, and overlapped at the sample within an area of 0.04 mm^2. The sum frequency (ω_{SF}) radiation was filtered by holographic notch filter and monochromator and detected by a photomultiplier tube and gated registration system. Typically, the signal was averaged over 100 pulses. However, in time-resolved experiments 60 pulses were co-added. On an average, the noise in these experiments was ∼12% of the signal intensity. SFG spectra were normalized according to intensity of infrared beam to take into account the changes in ω_{IR} energy with wavelength. The frequencies were calibrated by IR spectrum of polystyrene film placed in the path of the infrared beam. Two modes of SFG data acquiring were used. First, SFG spectra were collected by scanning of IR beam wavelength, and second SFG dynamics was observed by registering SFG signal changes in time at particular wavelength. To extract the parameters of SFG resonances, the experimental spectra have been fitted using eq 1[16]

$$I_{SFG} \propto \left| \chi^{(2)}_{NR} + \sum_n \frac{A_n e^{i\psi_n}}{\omega_{IR} - \omega_n + i\Gamma_n} \right|^2 \quad (1)$$

where I_{SFG} is the sum frequency intensity, $\chi^{(2)}_{NR}$ is the nonresonant contribution to the nonlinear susceptibility, and A_n, ψ_n, ω_n, and Γ_n are the strength, relative phase, resonant frequency, and line width of the nth vibration, respectively.

SFG experiments were conducted in a cylindrical glass cell, which was 38 mm in diameter. Before experiments, the cell was cleaned first with sodium hydroxide solution and subsequently with a mixture of concentrated nitric and sulfuric acid solutions. After these procedures, the cell was washed with ultrapure (Millipore purified) water. The cleanness of the cell and studied aqueous phase was checked by SFG spectroscopy (Figure S1, Supporting Information). No peaks in the C−H stretching region were detected before spreading the PDCHQ, which indicated absence of organic contaminants at studied solution/air interface.[17] SFG measurements were repeated 3−5 times by using newly prepared similar samples. The experiments were carried out at room (∼ 20 °C) temperature.

Millipore purified water (18.2 MΩ cm) was used throughout the work. PDCHQ was dissolved in diethyl ether (0.015 mM) and spread at the interface by placing a 100 μL drop on aqueous phase, containing 0.1 M NaCl and 0.01 M Na-phosphate buffer (pH 7.0), and the solvent was allowed to evaporate for 10 min. Higher PDCHQ concentrations were also used in preliminary SFG studies; however, because of lower signal reproducibility and stability the main investigations were performed at above indicated experimental conditions. Relatively low pH was used to minimize the spontaneous hydrolysis of PDCHQ.

Wild type (WT) TLL was obtained from Sigma (Germany; concentration 34.5 mg/mL as deduced from the UV absorption at 280 nm). S146A mutant of TLL was provided by Novozymes A/S (Bagsvaerd, Denmark) in a form of ca. 3−6 mg/mL solution. The purity of the enzyme was checked by SDS-PAGE.

Quantum chemical calculations were performed using Gaussian for Windows package version G03W.[18] The structure of the model compound, 2,3-dicyano-4-hydroxyphenyl propionate (DCHPP, Figure 1b), was optimized and the vibrational spectrum was calculated using density functional theory at B3LYP/6-311++G(2d,p) level. The calculated frequencies were not scaled.

3. Results and Discussion

3.1. Structure of PDCHQ Layer at Air/Water Interface. The studied lipid-like PDCHQ compound is composed of alkyl chain (14 methylene groups), ester linkage, and headgroup containing two CN and one OH moiety (Figure 1a). To get insight into the structure of adsorbed PDCHQ, it is important to acquire vibrational information not only from the alkyl chain part of the molecule but from the headgroup as well.[19,20] We were able to detect the SF resonances from both hydrophilic and hydrophobic parts of PDCHQ at the interface. Infrared and SFG spectra in the C≡N and C−H stretching regions of the studied compound are shown in Figure 2. Observation of well-expressed resonances indicates that the PDCHQ molecules adsorb at air/water interface in an ordered form.[15] Let us first consider the headgroup C≡N vibrational modes.

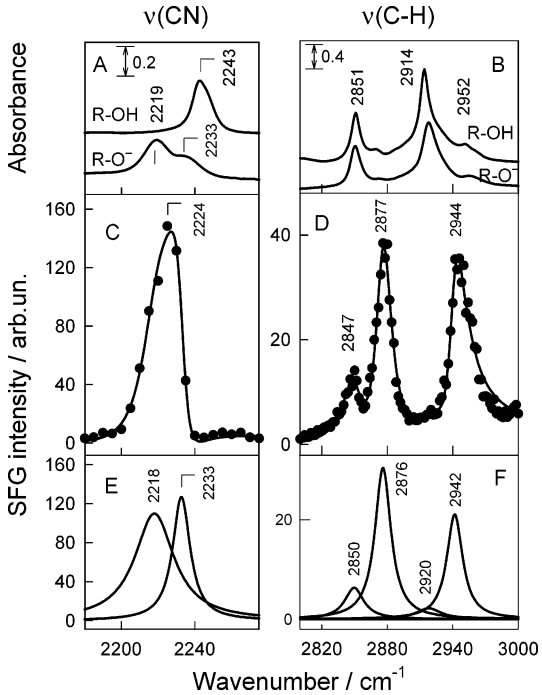

Figure 2. FT-IR spectra (A,B) of PDCHQ compound in the solid state (R-OH) and in the ionized state in aqueous solution (R-O$^-$), and SFG spectra (C,D) of PDCHQ at the air/water interface taken with ssp (s-SFG, s-532 nm, and p-IR) polarization combination. The solid lines (panels C and D) are fits to SFG spectra using Lorentzian functions. Panels E and F show vibrational modes constituting the SFG spectra. The phases of 2218 and 2233 cm^{-1} modes are 0 and π, respectively. The phases of modes in panel F are 0. The solution subphase is 0.1 M NaCl containing 0.01 M Na-phosphate buffer (pH 7.0).

C≡N Stretching Vibrations. Intense resonance due to the stretching vibration of CN groups emerges in the vicinity of 2224 cm^{-1} (Figure 2C). The pronounced peak asymmetry indicates interference effects between several resonances and background. Fitting experimental spectrum using eq 1 reveals the presence of two resonances located at 2218 and 2233 cm^{-1} (Figure 1E). Interpretation of SFG spectrum requires both experimental (IR and Raman) and theoretical analysis of C≡N vibrations in PDCHQ and similar compounds. Position of the C≡N stretching mode provides two-fold information: (i) hydrogen-bonding interaction of CN group at the interface[21−24] and (ii) ionization state of the OH group.[25,26] The interpretation of C≡N vibrations in studied PDCHQ is complicated because of the presence of two distinct cyano groups located at ortho (*o*-CN) and meta position (*m*-CN) from the hydroxyl-group. Previous studies of cyanophenols[25,26] have shown that the C≡N frequency for the isomers dissolved in DMSO decreases in the sequence: *m*-cyanophenol (2228 cm^{-1})[26] > *o*-cyanophenol (2223 cm^{-1})[25] > para (*p*)-cyanophenol (2221 cm^{-1}).[26] The effect has been related with polar resonance between the CN and OH groups.[26] Quantum chemical calculations performed with model compound DCHPP (Figure 1b) at B3LYP/6-311++G(2d,p) level predict *o*-CN and *m*-CN frequencies at 2310 and 2329 cm^{-1}, respectively. Table 1 summarizes the C≡N frequency shifts observed for PDCHQ compound in various environments along with the calculated values for model compound DCHPP. In the solid state, where PDCHQ forms C≡N•••H−O hydrogen bonds, FT-Raman and FT-IR spectra show intense *o*-CN peak at 2242 cm^{-1}. It is well known that C≡N stretching frequency blue shifts upon formation of hydrogen bond due to the reduction of the antibonding character and strengthening of the CN triple bond.[22,23] Indeed, for PDCHQ dissolved in an aprotic solvent, such as methylene chloride, the C≡N stretching vibration gives rise to a lower frequency peak at 2238 cm^{-1} (Table 1). Dissolving this compound in diethyl ether results in further red shift of the band to 2236 cm^{-1} (Table 1) This effect reflects the competitive action of diethyl ether that weakens the intramolecular hydrogen bonding[25,27] between the *o*-CN and OH groups.

Dramatic changes take place after ionization of the hydroxyl group; C≡N frequency considerably decreases and the second component of lower intensity became clearly visible in the IR spectrum (Figure 2A). Such red shift and increase in integrated intensity is characteristic for transformation of cyanophenols to oxyanions.[25,26] The pK_a value of PDCHQ dissolved in buffered aqueous solution containing 2% of Triton X-100 was estimated by UV−vis spectroscopy and was found to be 6.0 ± 0.2. Thus, in the studied solution of 0.1 M NaCl containing 0.01 M Na-phosphate buffer (pH 7.0), the ionized state of PDCHQ is expected to be dominant. However, at interface the pK_a value of amphiphiles in general might be different.[28] Therefore, the ionization state at the air/water interface needs to be determined independently. Positions of C≡N bands in the IR spectrum (2219 and 2233 cm^{-1}) are very close to the frequencies of two resonances obtained by fitting of the SFG spectrum (2218 and 2233 cm^{-1}, Figure 1 panels A and E, Table 1). In addition, narrowing of the higher frequency component at 2233 cm^{-1} compared to the 2218 cm^{-1} band was observed in both surface SFG (Figure 2E) and bulk FT-IR spectra (Figure S2, Supporting Information). Thus, our SFG spectra suggest that PDCHQ adsorbs at the interface predominantly in the ionized state and the *o*-CN group is hydrogen bonded with water molecules. The involvement of only one of the two CN groups in hydrogen-bonding interaction confirms observation of the different phases for 2233 and 2218 cm^{-1} components (Figure 2E) denoting that two CN groups point to different directions from the interface. However, we cannot completely discard some residual contribution to the 2233 cm^{-1} component from the C≡N vibrational mode in neutral PDCHQ molecules. Therefore, we can only safely conclude that the resonance at 2218 cm^{-1} belongs to the hydrogen-bonded *o*-CN group of the PDCHQ oxyanion.

C−H Stretching Vibrations. The C−H stretching region of SFG spectrum provides information on conformation and orientation of alkyl chains at interface.[6,29−35] The experimental SF spectrum of PDCHQ with nonlinear least-squares fit is shown in Figure 2D, and the vibrational modes constituting the spectrum are displayed in Figure 2F. For structural analysis of alkyl chains at molecular level, correct vibrational spectral interpretation is of fundamental importance. Recent systematic polarization analysis of the SFG spectra clarified the assignments of symmetric, asymmetric, and Fermi resonance C−H stretching modes and quantitative orientation evaluation of methine, methylene, and methyl groups at interface.[36−41] A pair of intense resonances at 2876 and 2942 cm^{-1} (Figure 2F) belongs to the CH_3 symmetric stretch (labeled r^+) and its Fermi resonance with an overtone of CH_3 bending mode (r^+_{FR}), respectively.[6,36,40,42] The CH_2 groups at interface can be recognized from the low-intensity symmetric stretch (d^+) at 2850 cm^{-1}.[40] This mode is clearly expressed in the infrared spectrum at 2851 cm^{-1} along with the intense CH_2 asymmetric stretching (d^-) peak at 2914 cm^{-1} (Figure 2B). In the presented interfacial spectrum, we were not able to observe the d^- mode. According to polarization selection rules,[40,41] the low-intensity resonance at 2920 cm^{-1} (Figure 2F) probably belongs to symmetric stretching Fermi resonance mode because of the same phase of this component

TABLE 1: Vibrational Frequencies (in cm^{-1}) for the C≡N Stretching Mode of PDCHQ in Various Environments

environment and state of the compound	method	CN group ortho-	CN group meta-
	PDCHQ		
solid powder	FT-IR	2242	2247 sh
solid powder	FT-Raman	2242	n.r.
methylene chloride	FT-IR	2238	n.r.
diethyl ether	FT-IR	2236	n.r.
model compound DCHPP in vacuum	calculated	2310	2329
	PDCHQ oxyanion		
solid powder, salt	FT-IR	2208	2237
aqueous solution, salt	ATR[a]-FT-IR	2219	2233
aqueous solution, 2% Triton X-100 + 0.1 M NaCl + 0.01 M Na-phosphate buffer (pH 8.0)	FT-IR	2216	2232
model compound DCHPP oxyanion	calculated	2247	2319
model compound DCHPP oxyanion, Na^+, $2H_2O$[b]	calculated	2261	2318
air/water interface	SFG	2218 ± 3	2233 ± 3

[a] attenuated total reflection. [b]Calculations were performed for model compound DCHPP oxyanion with Na^+ and two H_2O molecules. Abbreviations: sh, shoulder; n.r., not resolved

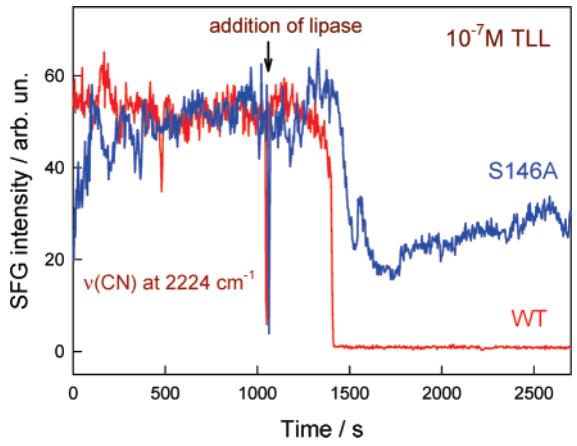

Figure 3. Time dependence of the intensity of SFG resonance for PDCHQ C≡N stretch at 2224 cm^{-1} after addition of 10^{-7} M WT TLL and its S146A mutant.

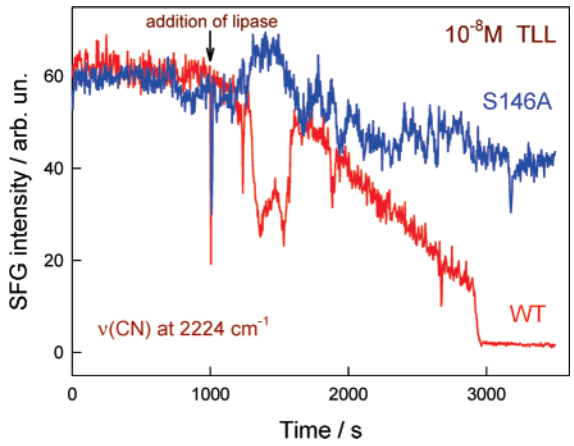

Figure 4. Time dependence of the intensity of SFG resonance for PDCHQ C≡N stretch at 2224 cm^{-1} after addition of 10^{-8} M WT TLL and its S146A mutant.

as d^+ resonance. SFG spectroscopy is extremely sensitive to conformational and orientation changes of molecules at interfaces due to the lack of inversion symmetry selection rule.[15,19] Because of the cancellation of contributions from the d^+ modes due to the opposite dipoles with respect to carbon backbone, the SF spectrum of ordered all-trans hydrocarbon chains of lipids with an even number of methylene groups at interfaces is dominant by the methyl bands.[4,6,19,42] Gauche defects destroy local symmetry causing an increase of a CH_2 signal intensity. Therefore, the SF spectral intensity ratio $\rho = A_{r+}/A_{d+}$ is recognized as a parameter characterizing the conformational order of alkyl chains.[42,43] In our case, ρ value for PDCHQ was found to be 1.8 ± 0.2, which is comparable to the well-organized adlayer of dodecylammonium chloride ($\rho = 1.6$) at D_2O/CCl_4 interface (5 mM bulk concentration),[6] and dilauroylphosphatidylcholine (DLPC, $\rho = 1.9$)[43] layer at air/water interface. However, considerably higher ρ values were observed for longer chain dipalmitoylphosphatidylcholine (DPPC, $\rho = 5.3$) and distearoylphosphatidylcholine (DSPC, $\rho = 11.9$) monolayers at air/water interface.[43] Obtained in this work, the A_{r+}/A_{d+} ratio for PDCHQ suggests liquidlike state of the monolayer.[44]

3.2. Decay of CN Resonance after Injection of Enzyme. Real time variation of the intensity of C≡N resonance (2224 cm^{-1}) after the injection of TLL into the subphase is demonstrated in Figure 3. Because of relatively low accumulation (60 pulses/point), the time-dependent curves are rather noisy. Without lipase, the C≡N vibrational signal was found to be relatively stable in the studied time scale. After the addition of WT enzyme, the C≡N band remains stable for some time and then starts decaying. As seen from Figure 3, at some point of time, which is dependent on TLL concentration, the decay curve abruptly drops to the background level. Such a steep SF signal decrease might be associated with the collapse of monolayer due to the enzymatic hydrolysis of PDCHQ or/and the strong perturbation of monolayer's order by the enzyme adsorption. To differentiate these effects, we employed the inactivated S146A mutant of TLL. It is known that the hydrolytic activity of TLL is determined by the catalytic triad of amino acids Ser-His-Asp.[45,46] Replacement of Ser146 in the catalytic triad with alanine (S146A mutant)[47] results in ~500 times lower hydrolytic activity.[48] As can be seen from Figure 3, the addition of S146A mutant at 10^{-7} M concentration does not trigger total C≡N resonance disappearance as in the case of the WT enzyme. Instead, an approximately 60% drop in signal intensity was detected. These results indicate a disruption of ordering of CN dipoles at interface due to the penetration of enzyme into the monolayer. If the protein-induced disordering effect dominates, it must be sensitive to the enzyme concentration. Figure 4 shows the time-dependence of intensity of the C≡N resonance after introduction of WT and S146A mutant TLL at 10^{-8} M concentration. Reduction of WT enzyme concentration results in two effects: (i) the initial slope of signal decay markedly

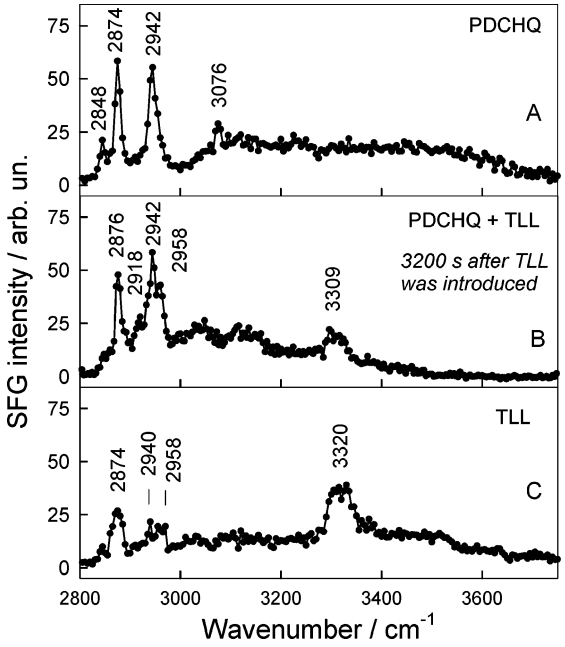

Figure 5. SFG spectra of (A) PDCHQ at air/water interface, (B) 3200 s after 10^{-6} M TLL was introduced, and (C) TLL (10^{-6} M) at air/water interface taken with ssp (s-SFG, s-532 nm, and p-IR) polarization combination. The solid lines are guides to the eye. The subphase consists of 0.1 M NaCl and 0.01 M Na-phosphate buffer (pH 7.0).

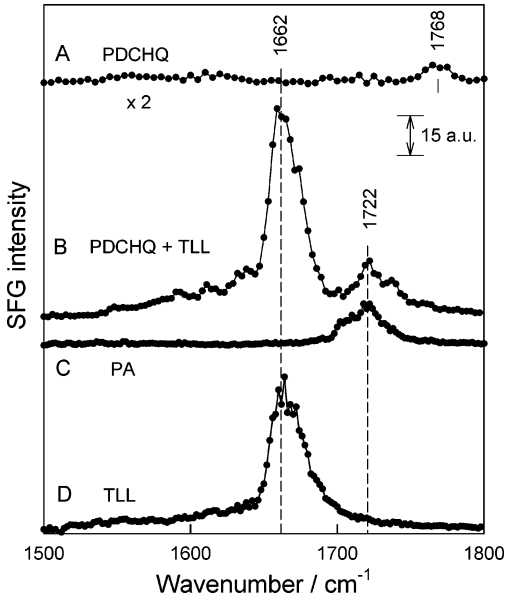

Figure 6. SFG spectra of (A) PDCHQ at air/water interface, (B) 3200 s after 10^{-6} M TLL was introduced, (C) palmitilic acid (PA), and (D) lipase (10^{-6} M) at air/water interface taken with ssp (s-SFG, s-532 nm, and p-IR) polarization combination. The solid lines are guides to the eye. The subphase consists of 0.1 M NaCl and 0.01 M Na-phosphate buffer (pH 7.0).

decreases, and (ii) the time required to fully destroy the CN signal by the WT lipase increases from 400 to 2000 s. On the other hand, the reduction of S146A mutant concentration results in much smaller (of ~20%) decline of C≡N signal. These results prove that enzymatic cleavage indeed takes place at the studied interface. Obvious perturbations of the C≡N mode intensity versus time curve, which starts appearing after 200−600 s after the enzyme injection (Figure 4), are presumably due to the adsorption of lipase at interface and interaction with the PDCHQ layer. It is well documented that activity of lipases increases sharply upon binding to the interfaces of lipid aggregates.[49] The interfacial activation mechanism is not fully understood at present, and it is a subject of intense research.[50,51] It should be noted, that while perturbations in 200−600 s interval after the TLL (10^{-8} M) injection was observed for all studied samples, these changes were not regular. The most reproducible features in the time-dependent experiments were found to be the time required to decrease the CN signal intensity to zero in the case of WT enzyme, and the residual signal intensity level for the mutant TLL. Both parameters depend on the enzyme concentration (Figures 3 and 4).

3.3. Adsorption of Lipase at Interface. Direct evidence of lipase penetration into the PDCHQ monolayer was obtained by the analysis of 2800−3750 (Figure 5) and 1500−1800 cm^{-1} (Figure 6) frequency intervals. Lipase-induced spectral changes in the high-frequency range are shown in Figure 5B. Two clearly expressed resonances at 2876 and 2942 cm^{-1} associated with r^+ and r^+_{FR} vibrational modes, respectively, indicate presence of ordered alkyl chains at interface. These resonances probably belong to the stretching modes of the terminal CH_3 group of the hydrolysis product ($CH_3(CH_2)_{14}COOH$) present at interface. However, the additional shoulders due to d^-/d^+_{FR} and r^-/d^+_{FR} modes emerge at 2918 and 2958 cm^{-1}, respectively.[40] The asymmetric methylene (d^-) and methyl (r^-) stretching modes are clearly visible in the sps polarized spectrum (Figure S4, Supporting information) near 2920 and 2966 cm^{-1}.[40,41] It should be noted that d^- component was not observed in sps spectrum of PDCHQ monolayer (Figure S3, Supporting information), and the relative intensity of the r^- component increases in the spectrum recorded in the presence of TLL. This observation implies orientational changes of the alkyl chains of hydrolysis product palmitic acid or/and SF resonance contributions from the amino acid residues of the enzyme. Indeed, C−H resonances from TLL at air/water interface are clearly visible in the 2800−3000 cm^{-1} spectral region (Figure 5C). We assume that the main contribution to the C−H spectrum comes from the interference of lipase signals. However, definitive separation of contribution from different species is only possible by SFG analysis of perdeuterated PDCHQ.[52] It should be noted that sharp and weak resonance at 3076 cm^{-1} (Figure 5A) due to the C−H stretching vibration of PDCHQ ring disappears upon incubation with lipase (Figure 5B). In addition, marked decrease in intensity of a broad water band in the frequency region of 3400−3600 cm^{-1} is observed. It should be noted that SF signal intensity of broad water bands in Figure 5A is enhanced by a factor of ~7 as compared with pure water spectrum in agreement with well-documented enhancement of water modes for charged organic monolayers at air/water interface due to the electric field-induced alignment of H_2O molecules.[53] These two effects suggest that hydrophilic (charged) part of PDCHQ leaves surface region after the hydrolysis, while the hydrophobic part of the molecule remains at the air/water interface.

However, one of the most striking observations is the appearance of a distinct feature in the vicinity of 3309 cm^{-1} (Figure 5B), which might be associated with the presence of TLL at the interface.

To probe whether or not lipase is responsible for this feature of the SFG spectrum, we investigated air/water interface of buffered aqueous solution containing only enzyme (no PDCHQ) in the subphase (Figure 5C). In the C−H stretching region, the broad r^+ peak at 2874 cm^{-1} along with the lower intensity d^- and r^- resonances at 2940 and 2958 cm^{-1}, respectively, were detected. These modes are presumably associated with the C−H stretching vibrations of TLL amino acid residues and attest for the presence of the enzyme at interface.[10] Following Jung et

al.[54] who detected the N−H band at 3280 cm^{-1} in SFG spectrum of adsorbed fibrinogen on silica substrate, we tentatively assign the broad feature at ∼3320 cm^{-1} to N−H stretching vibration. In our opinion, an intense 3320-cm^{-1} resonance indicates the existence of aligned N−H bonds of the adsorbed enzyme. Indirect confirmation of this assumption comes from the analysis of 1500−1800 cm^{-1} frequency region.

In the middle frequency interval (Figure 6A) before introduction of lipase, low-intensity resonance at 1768 cm^{-1} due to the C═O stretching vibration of PDCHQ ester bond was observed. This mode was detected at 1769 cm^{-1} in FT-IR spectrum of the potassium salt of PDCHQ oxyanion pressed in KBr. In the SFG spectrum recorded 3200 s after the injection of TLL (Figure 6B), the ester band disappears and an intense feature centered at 1662 cm^{-1} along with the lower intensity resonance at 1722 cm^{-1} shows up. It is reasonable to expect that the SF signal originating from the hydrolysis product should be observed in the spectrum B of Figure 6. To determine the spectral characteristics of hydrolysis product, we recorded SFG spectrum from the subphase without the enzyme and PDCHQ but with spread palmitic acid (Figure 6C). This spectrum is dominated by the clear resonance at 1722 cm^{-1} due to the C═O stretching mode of protonated carboxyl group[53,55−57] of palmitic acid. Comparison of spectra B and C reveals that the 1722 cm^{-1} peak belongs to the hydrolysis product of PDCHQ. Frequency of this mode is sensitive to hydrogen-bonding interaction. Infrared reflection−absorption spectroscopic studies of fatty acids at air/water interface[56,57] have shown that three C═O stretching bands located in the 1734−1739, 1715−1722, and 1700−1704 cm^{-1} frequency intervals originate from the non-hydrogen-bonded, singly hydrogen-bonded, and doubly hydrogen-bonded carbonyl groups, respectively. Thus, our SF spectrum in Figure 6B indicates that upon enzymatic hydrolysis of PDCHQ the headgroup of palmitic acid is hydrogen-bonded at air/water interface. To assess the origin of the intense 1662 cm^{-1} resonance (Figure 6B), we acquired the SF spectrum from the subphase without PDCHQ but containing 10^{-6} M of TLL (Figure 6D). The observed intense peak at 1663 cm^{-1} due to the presence of TLL is similar to that detected in the spectrum of Figure 6B, thus attesting our presumption that after the hydrolysis along with the palmitic acid the air/water interface is also populated by the enzyme molecules.

Let us consider the assignment of 1662 cm^{-1} band. This feature falls into the frequency region (1610−1695 cm^{-1}) characteristic for a particular vibration of protein amide linkages called amide I mode.[58] The main contribution for amide I vibration comes from the backbone C═O stretching motion (83%) coupled with an out-of-phase C−N stretching and C−C−N deformation,[59] therefore frequency of this mode is sensitive to the secondary structure of polypeptide chains.[58−61] TLL is a 269 amino acid residue enzyme[62] and according to X-ray diffraction data it consists of a single spherical domain with the central sheet composed of eight predominantly parallel β-pleated sheets with five interconnecting α-helixes.[63] The contents of α-helixes, β-sheets and turns, and 3_{10}-helixes determined by X-ray crystallography were found to be 26, 26, and 7% of the overall amide bonds, respectively.[64] Recently, amide I signals have been detected by SFG spectroscopy at solid/liquid interfaces,[65−68] and α-helix, β-sheet, turns, and disordered structures of interfacial proteins were distinguished. From its position, the dominant 1662 cm^{-1} peak in the SFG spectrum must be related with C═O groups involved in weak hydrogen-bonding characteristic for β-turns, random structures, or 3_{10}-helixes.[58]

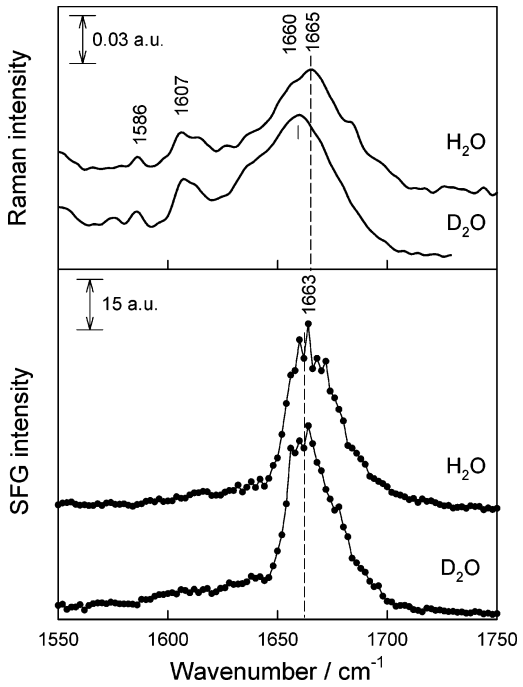

Figure 7. FT-Raman spectra of TLL in 0.02 M Na-phosphate buffer (pH 7.5) and SFG spectra of TLL at air/water interface for the H_2O- and D_2O-based solutions. SFG spectra were taken with ssp (s-SFG, s-532 nm, and p-IR) polarization combination. The subphase consists of 0.1 M NaCl and 0.01 M Na-phosphate buffer (pH 7.0). The solid lines are guides to the eye. SFG spectrum in D_2O solution was recorded 2 h after 10^{-6} M TLL was introduced into the subphase.

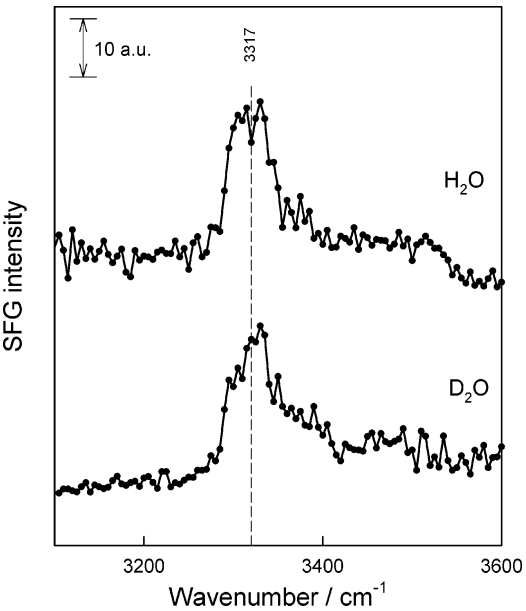

Figure 8. SFG spectra of TLL at air/water interface for solutions prepared with H_2O and D_2O. Spectra were taken with ssp (s-SFG, s-532 nm, and p-IR) polarization combination. The solid lines are guides to the eye. The subphase consists of 0.1 M NaCl, 0.01 M Na-phosphate buffer (pH 7.0), and 10^{-6} M TLL. SFG spectrum of TLL at air/D_2O interface was recorded after 2 h incubation in the enzyme-containing subphase.

To further access the nature of TLL bands observed by SFG spectroscopy, we performed solution isotopic H_2O/D_2O exchange experiments (Figures 7 and 8). No frequency shifts were detected for both amide I (Figure 7) and high-frequency 3317 cm^{-1} (Figure 8) bands after 2 h of incubation with TLL in D_2O compared to H_2O. It should be noted that contrary to SF signal collected from air/water interface, the amide I mode in the FT-

Raman spectrum of TLL solution clearly shifts to lower wavenumbers by ~5 cm^{-1} upon H_2O substitution with D_2O (Figure 7). The observed difference in H/D exchange is explained by the fact that FT-Raman spectroscopy examines the secondary structure of the entire enzyme molecule in solution, and the SFG technique probes only the certain fragments of enzyme secondary structure, that is, aligned amide bonds at interface. In addition, transformation in secondary structure is expected upon adsorption of lipase at interface.[50,51] Previous FT-IR spectroscopic analysis of TLL in solution revealed exchange of 63% of peptide CONH groups to COND during 2 h required to achieve the equilibrium.[69] The isotopic exchange was also observed for enzyme adsorbed at solid hydrophobic surface and was explained by assuming that adsorbed lipase adopts open conformation. It has been demonstrated[70] that for peptides with predominant random structures of amide linkages, fast H/D exchange process takes place. Thus, random structures can be excluded as possible sources of observed resonances. Our results suggest that β-turns are probably responsible for the peak at 1662 cm^{-1}. The β-turns consisting of four amino acid residues with or without internal hydrogen bonding are the third important structural elements in addition to α-helixes and β-sheets, which determine the three-dimensional structure of globular proteins.[71,72] The N−H stretching vibration (amide A) of the same type amide groups most likely gives rise to the high-frequency resonance in the vicinity of 3320 cm^{-1}. For TLL in aqueous solution, the amide A band in the FT-IR spectrum was observed at lower wavenumbers (3280 cm^{-1}). Increase in frequency for this mode in SF spectrum indicates that N−H bonds are involved in relatively weak hydrogen-bonding interaction. The absence of the H/D exchange within 2 h after the injection of enzyme into the D_2O-based subphase (Figure 8) suggests that amide groups responsible for the SFG signal are buried inside the hydrophobic region of TLL.

4. Conclusions

This study presents a step toward the in situ real-time monitoring of the interfacial enzymatic processes by the nonlinear sum-frequency generation technique. We have probed enzymatic activity of triglyceride hydrolase (EC 3.1.1.3) *Thermomyces lanuginosus* lipase at air/water interface in the broad infrared frequency region (1500−3750 cm^{-1}). As a substrate, we have used the newly synthesized amphiphilic compound, O-palmitoyl-2,3-dicyanohydroquinone composed of long alkyl chain, ester linkage required for enzyme action, OH moiety, and two CN groups serving as vibrational markers because of high SFG activity and comfortable frequency region, free from overlapping with any C−H or ring vibrations. Previously,[14] using electrochemical methods, we have demonstrated that this compound is enzymatically cleaved by TLL. The structure of adsorbed PDCHQ was probed by SFG in hydrophobic (C−H) and headgroup (C−N) frequency regions. Analysis of the intensity ratio of methyl and methylene symmetric stretching resonances ($A_{r+}/A_{d+} = 1.8 \pm 0.2$) has revealed a high degree of conformational order of alkyl chains and a relatively low number of gauche defects. In the headgroup region, the asymmetric SF signal centered at 2224 cm^{-1} was fitted by two components at 2218 and 2233 cm^{-1}, which were assigned to C≡N resonances of *o*-CN and *m*-CN groups, respectively. From the C≡N vibrational frequency, it was identified that OH group of PDCHQ exists predominantly in the ionized state, and the CN groups are hydrogen-bonded with water molecules. We have observed the decrease in intensity of well-defined CN signal at 2224 cm^{-1} after introduction of TLL into the subphase. Comparison of time dependence of the intensity of CN signal for WT and inactive S146A TLL mutant at different protein concentrations allowed us to conclude that two processes occur at the interface: protein adsorption-induced disordering of the monolayer and enzymatic cleavage of the ester bond. The high sensitivity of SFG technique was demonstrated by the observation of decay of CN resonance at the concentration of enzyme as low as 10 nM. The adsorption of lipase in the ordered form at interface was spectroscopically confirmed by the observation of SF signals in the amide I (1662 cm^{-1}) and amide A (3320 cm^{-1}) frequency regions. On the basis of H/D exchange experiments performed in D_2O, it was suggested that protein SF resonances are associated with aligned amide groups buried inside the hydrophobic domain. Our data suggest the possibility of utilizing SFG spectroscopy as a tool to a real-time monitoring of enzymatic activity at the air/water interface.

Acknowledgment. Financial support from the European Community under contract NMP4-CT-2003-505211 is gratefully acknowledged. The authors thank Dr. Olegas Eicher-Lorka (Vilnius) for vibrational analysis of model compound.

Supporting Information Available: Experimental details, analysis of C≡N stretching vibrations, Figures S1−S4. This information is available free of charge via the Internet at http://pubs.acs.org.

References and Notes

(1) Beisson, F.; Tiss, A.; Rivière, C.; Verger, R. *Eur. J. Lipid Sci. Technol*. **2000**, 133−153.
(2) Piéroni, G.; Gargouri, Y.; Sarda, L.; Verger, R. *Adv. Colloid Interface Sci*. **1990**, *32*, 341−378.
(3) Schmid, R. D.; Verger, R. *Angew. Chem., Int. Ed*. **1998**, *37*, 1609−1633.
(4) Guyot-Sionnest, P.; Hunt, J. H.; Shen, Y. R. *Phys. Rev. Lett*. **1987**, *59*, 1597−1600.
(5) Shen, Y. R. *Solid State Commun.* **1997**, *102*, 221−229.
(6) Conboy, J. C.; Messmer, M. C.; Richmond, G. L. *J. Phys. Chem. B* **1997**, *101*, 6724−6733.
(7) Roke, S.; Schins, J.; Muller, M.; Bonn, M. *Phys. Rev. Lett*. **2003**, *90*, 128101.
(8) Gurau, M. C.; Castellana, E. T.; Albertorio, F.; Kataoka, S.; Lim, S.-M.; Yang, R. D.; Cremer, P. S. *J. Am. Chem. Soc*. **2003**, *125*, 11166−11167.
(9) Hore, D. K.; Beaman, D. K.; Richmond, G. L. *J. Am. Chem. Soc*. **2005**, *127*, 9356−9357.
(10) Chen, X.; Clarke, M. L.; Wang, J.; Chen, Z. *Int. J. Modern Phys. B* **2005**, *19*, 691−713.
(11) Kim, G.; Gurau, M.; Kim, J.; Cremer, P. S. *Langmuir* **2002**, *18*, 2807−2811.
(12) Kim, G.; Gurau, M. C.; Lim, S.-M.; Cremer, P. S. *J. Phys. Chem. B* **2003**, *107*, 1403−1409.
(13) Berg, O. G.; Cajal, Y.; Butterfoss, G. L.; Ascunion Alsina, M.; Yu, B.-Z.; Jain, M. K. *Biochemistry* **1998**, *37*, 6615−6627.
(14) Ignatjev, I.; Valincius, G.; Švedaitė, I.; Gaidamauskas, E.; Kažemėkaitė, M.; Razumas, V.; Svendsen, A. *Anal. Biochem*. **2005**, *344*, 275−277.
(15) Richmond, G. L. *Chem. Rev*. **2002**, *102*, 2693−2724.
(16) Miranda, P. B.; Shen, Y. R. *J. Phys. Chem. B* **1999**, *103*, 3292−3307.
(17) Gragson, D. E.; McCarty, B. M.; Richmond, G. L. *J. Am. Chem. Soc*. **1997**, *119*, 6144−6152.
(18) Frisch, M. J.; Trucks, G. W.; Schlegel, H. B.; Scuseria, G. E.; Robb, M. A.; Cheeseman, J. R.; Montgomery, J. A., Jr.; Vreven, T.; Kudin, K. N.; Burant, J. C.; Millam, J. M.; Iyengar, S. S.; Tomasi, J.; Barone, V.; Mennucci, B.; Cossi, M.; Scalmani, G.; Rega, N.; Petersson, G. A.; Nakatsuji, H.; Hada, M.; Ehara, M.; Toyota, K.; Fukuda, R.; Hasegawa, J.; Ishida, M.; Nakajima, T.; Honda, Y.; Kitao, O.; Nakai, H.; Klene, M.; Li, X.; Knox, J. E.; Hratchian, H. P.; Cross, J. B.; Bakken, V.; Adamo, C.; Jaramillo, J.; Gomperts, R.; Stratmann, R. E.; Yazyev, O.; Austin, A. J.; Cammi, R.; Pomelli, C.; Ochterski, J. W.; Ayala, P. Y.; Morokuma, K.; Voth, G. A.; Salvador, P.; Dannenberg, J. J.; Zakrzewski, V. G.; Dapprich, S.; Daniels, A. D.; Strain, M. C.; Farkas, O.; Malick, D. K.; Rabuck, A. D.; Raghavachari, K.; Foresman, J. B.; Ortiz, J. V.; Cui, Q.; Baboul, A.

G.; Clifford, S.; Cioslowski, J.; Stefanov, B. B.; Liu, G.; Liashenko, A.; Piskorz, P.; Komaromi, I.; Martin, R. L.; Fox, D. J.; Keith, T.; Al-Laham, M. A.; Peng, C. Y.; Nanayakkara, A.; Challacombe, M.; Gill, P. M. W.; Johnson, B.; Chen, W.; Wong, M. W.; Gonzalez, C.; Pople, J. A. *Gaussian 03*, revision D.01; Gaussian, Inc.: Wallingford, CT, 2004.

(19) Ma, G.; Allen, H. C. *Langmuir* **2006**, *22*, 5341−5349.

(20) Zhang, D.; Gutow, J.; Eisenthal, K. B. *J. Phys. Chem.* **1994**, *98*, 13729−13734.

(21) Reimers, J. R.; Hall, L. E. *J. Am. Chem. Soc.* **1999**, *121*, 3730−3744.

(22) Getahun, Z.; Huang, C.-Y.; Wang, T.; De León, B.; DeGrado, W. F.; Gai, F. *J. Am. Chem. Soc.* **2003**, *125*, 405−411.

(23) Chaban, G. M. *J. Phys. Chem. A* **2004**, *108*, 4551−4556.

(24) Soule, M. C. K.; Hore, D. K.; Jaramillo-Fellin, D. M.; Richmond, G. L. *J. Phys. Chem. B* **2006**, *110*, 16575−16583.

(25) Binev, Y. I.; Georgieva, M. K.; Daskalova, L. I. *Spectrochim. Acta* **2004**, *60A*, 2601−2610.

(26) Georgieva, M. K.; Angelova, P. N.; Binev, I. G. *J. Mol. Struct.* **2004**, *692*, 23−35.

(27) Broquier, M.; Lahmani, F.; Zehnacker-Rention, A.; Brenner, V.; Millie, Ph.; Peremans, A. *J. Phys. Chem. A* **2001**, *105*, 6841−6850.

(28) Ouimet, J.; Croft, S.; Pare, C.; Katsaras, J.; Lafleur, M. *Langmuir* **2003**, *19*, 1089−1097.

(29) Bell, G. R.; Bain, C. D.; Ward, R. N. *J. Chem. Soc., Faraday Trans.* **1996**, *92*, 515−523.

(30) Watanabe, N.; Yamamoto, H.; Wada, A.; Domen, K.; Hirose, C. *Spectrochim. Acta* **1994**, *50A*, 1529−1537.

(31) Ye, S.; Morita, S.; Li, G.; Noda, H.; Tanaka, K.; Uosaki, K.; Osawa, M. *Macromolecules* **2003**, *36*, 5694−5703.

(32) Ye, S.; Noda, H.; Nishida, T.; Morita, S.; Osawa, M. *Langmuir* **2004**, *20*, 357−365.

(33) Zhuang, X.; Miranda, P. B.; Kim, D.; Shen, Y. R. *Phys. Rev. B* **1999**, *59*, 12632−12640.

(34) Conboy, J. C.; Messmer, M. C.; Richmond, G. L. *J. Phys. Chem.* **1996**, *100*, 7617−7622.

(35) Zhang, D.; Ward, R. S.; Shen, Y. R.; Somorjai, G. A. *J. Phys. Chem. B* **1997**, *101*, 9060−9064.

(36) Gan, W.; Wu, B. H.; Zhang, Z.; Guo, Y.; Wang, H. F. *J. Phys. Chem. C* **2007**, *111*, 8716−8725.

(37) Gan, W.; Zhang, Z.; Feng, R. R.; Wang, H. F. *J. Phys. Chem. C* **2007**, *111*, 8726−8738.

(38) Gan, W.; Zhang, Z.; Feng, R. R.; Wang, H. F. *Chem. Phys. Lett.* **2006**, *423*, 261−265.

(39) Wang, H. F.; Gan, W.; Lu, R.; Rao, Y.; Wu, B. H. *Int. Rev. Phys. Chem.* **2005**, *24*, 191−256.

(40) Lu, R.; Gan, W.; Wu, B. H.; Zhang, Z.; Guo, Y.; Wang, H. F. *J. Phys. Chem. B* ***2005***, *109*, 14118−14129.

(41) Lu, R.; Gan, W.; Wu, B. H.; Chen, H.; Wang, H. F. *J. Phys. Chem. B* **2004**, *108*, 7297−7306.

(42) Gragson, D. E.; McCarty, B. M.; Richmond, G. L. *J. Am. Chem. Soc.* **1997**, *119*, 6144−6152.

(43) Walker, R. A.; Gruetzmacher, J. A.; Richmond, G. L. *J. Am. Chem. Soc.* **1998**, *120*, 6991−7003.

(44) Varga, I.; Keszthelyi, T.; Mészaros, R.; Hakkel, O.; Gilanyi, T. *J. Phys. Chem. B* **2005**, *109*, 872−878.

(45) Svendsen, A. *Biochim. Biophys. Acta* **2000**, *1543*, 223−238.

(46) Brady, L.; Brzozowski, A. M.; Derewenda, Z. S.; Dodson, E.; Dodson, G.; Tolley, S.; Turkenburg, J. P.; Christiansen, L.; Huge-Jensen, B.; Norskov, L.; Thim, L.; Menge, U. *Nature* **1990**, *343*, 767−770.

(47) Peters, G. H.; Svendsen, A.; Laugberg, H.; Vind, J.; Patkar, S. A.; Kinnunen, P. K. *J. Colloids Surf. B* **2002**, *26*, 123−134.

(48) Svendsen, A. Novozymes A/S, Bagsvaerd, Denmark. Unpublished data.

(49) Sarda, L.; Desnuelle, P. *Biochim. Biophys. Acta* **1958**, *30*, 513−521.

(50) Cajal, Y.; Svendsen, A.; Girona, V.; Patkar, S. A.; Alsina, M. A. *Biochemistry* **2000**, *39*, 413−423.

(51) Hedin, E. M. K.; Høyrup, P.; Patkar, S. A.; Vind, J.; Svendsen, A.; Hult, K. *Biochemistry* **2005**, *44*, 16658−16671.

(52) Holman, J.; Davies, P. B.; Neivandt, D. J. *J. Phys. Chem. B* **2004**, *108*, 1396−1404.

(53) Miranda, P. B.; Du, Q.; Shen, Y. R. *Chem. Phys. Lett.* **1998**, *286*, 1−8.

(54) Jung, S. Y.; Lim, S. M.; Albertorio, F.; Kim, G.; Gurau, M. C.; Yang, R. D.; Holden, M. A.; Cremer, P. S. *J. Am. Chem. Soc.* **2003**, *125*, 12782−12786.

(55) Stefan, I. C.; Mandler, D.; Scherson, D. A. *Langmuir* **2002**, *18*, 6976−6980.

(56) Johann, R.; Vollhardt, D.; Möhwald, H. *Colloids Surf., A* **2001**, *182*, 311−320.

(57) Gericke, A.; Hühnerfuss, H. *J. Phys. Chem.* **1993**, *97*, 12899−12908.

(58) Jackson, M.; Mantsch, H. H. *Crit. Rev. Biochem. Mol. Biol.* **1995**, *30*, 95−120.

(59) Krimm, S.; Bandekar, J. *Adv. Protein Chem.* **1986**, *38*, 181−364.

(60) Kirsch, J.; Koenig, J. L. *Appl. Spectrosc.* **1989**, *43*, 445−451.

(61) Torreggiani, A.; Fini, G. *J. Raman Spectrosc.* **1999**, *30*, 295−300.

(62) Martinelle, M.; Holmquist, M.; Hult, K. *Biochim. Biophys. Acta* **1995**, *1258*, 272−276.

(63) Derewenda, U.; Swenson, L.; Green, R.; Wei, Y.; Dodson, G. G.; Yamaguchi, S.; Haas, M. J.; Derewenda, Z. S. *Protein Eng.* **1994**, *7*, 551−557.

(64) Lawson, D. M.; Brzozowski, A. M.; Rety, S.; Verma, C.; Dodson, G. G. *Protein Eng.* **1994**, *7*, 543−550.

(65) Wang, J.; Even, M. A.; Chen, X.; Schmaier, A. H.; Waite, J. H.; Chen, Z. *J. Am. Chem. Soc.* **2003**, *125*, 9914−9915.

(66) Wang, J.; Clarke, M. L.; Chen, X.; Even, M. A.; Johnson, W. C.; Chen, Z. *Surf. Sci.* **2005**, *587*, 1−11.

(67) Chen, X.; Wang, J.; Sniadecki, J. J.; Even, M. A.; Chen, Z. *Langmuir* **2005**, *21*, 2662−2664.

(68) Clarke, M. L.; Wang, J.; Chen, Z. *J. Phys. Chem. B* **2005**, *109*, 22027−22035.

(69) Noinville, S.; Revault, M.; Baron, M.-H.; Tiss, A.; Yapoudjian, S.; Ivanova, M.; Verger, R. *Biophys. J.* **2002**, *82*, 2709−2719.

(70) Susi, H.; Timasheff, S. N.; Stevens, L. *J. Biol. Chem.* **1967**, *242*, 5460−5466.

(71) Mantsch, H. H.; Perczel, A.; Hollósi, M.; Fasman, G. D. *Biopolymers* **1993**, *33*, 201−207.

(72) Perczel, A.; Hollósi, M.; Foxman, B. M.; Fasman, G. D. *J. Am. Chem. Soc.* **1991**, *113*, 9772−9784.